The 5th Joint International Conference on Multibody System Dynamics
June 24 –28, 2018, Lisbon, Portugal

Mathematical modelling of spatial linkages with clearance, friction and links' flexibility effects

Krzysztof Augustynek, Andrzej Urbaś

Department of Mechanical Engineering Fundamentals, University of Bielsko-Biala, {kaugustynek,aurbas}@ath.bielsko.pl

ABSTRACT — *The paper presents mathematical model of the spatial linkages with flexible links, clearance and friction effects in joints. In the general case kinematic structure the linkage can be open- or closed-loop. Open-loop systems can form serial or tree structure. When closed-loop kinematic chains are analysed, it is necessary to convert such a system into an equivalent system with an open-loop kinematic structure. The cut-joint technique is used to make such conversion. The joint coordinates and homogeneous transformation matrices are used in description of the motion of the system. The flexibility of links is modelled by means of the Rigid Finite Element Method. It is assumed that joints are imperfect i.e. the clearance and friction in joints are taken into account. It is assumed that the clearance exists only in rotational joints, and two models of the clearance, planar and spatial, are proposed. The LuGre bristles' friction model is used. The dynamics equations of motion of the linkage are derived using the Lagrange's equations. These equations are supplemented with closing constraints equations, formulated for joints in which closed-loop chains are cut. As an example a one-dof spatial RSUP linkage is analysed.*

Nomenclature

g – acceleration of gravity,
c – symbol of chain
l – symbol of link,
$\mathrm{rfe}(c,l,r)$ – symbol of r-th rigid finite element of link l in chain c,
$\mathrm{sde}(c,l,s)$ – symbol of s-th spring-damping element of link l in chain c,
$l^{(c,l)}$ – length of link l in chain c,
$l^{(c,l,r)}$ – length of r-th rigid finite element of link l in chain c,
$m^{(c,p)}$ – mass of link l in chain c,
$n_{dof}^{(c)}$ – number of generalized coordinates describing the motion of chain c with respect to the reference system $\{0\}$,
$\tilde{n}_{dof}^{(c,l)}$ – number of generalized coordinates describing the motion of link l with respect to link $l-1$ in chain c,
$n_{dof}^{(c,l)}$ – number of generalized coordinates describing the motion of link l in chain c with respect to the reference system $\{0\}$,
$n_{sde}^{(c,l)}$ – number of sdes of link l in chain c,
$n_{rfe}^{(c,l)}$ – number of rfes of link l in chain c,
$n_{l}^{(c)}$ – number of links in chain c,

$\tilde{\mathbf{q}}^{(c,l)}$ – vector of generalized coordinates describing the motion of link l with respect to link $l-1$, $\tilde{\mathbf{q}}^{(c,l)}\Big|_{\substack{c=1,2\\ l=1,\dots,n_l^{(c)}}} = \left(\tilde{q}_j^{(c,l)}\right)_{j=1,\dots,\tilde{n}_{dof}^{(c,l)}}$,

$\mathbf{q}^{(c,l)}$ – vector of generalized coordinates describing the motion of link l with respect to the reference system $\{0\}$, $\mathbf{q}^{(c,l)}\Big|_{\substack{c=1,2\\ l=1,\dots,n_l^{(c)}}} = \left(q_j^{(c,l)}\right)_{j=1,\dots,n_{dof}^{(c,l)}}$,

$\tilde{\mathbf{T}}^{(c,l)}$ – homogeneous transformation matrix from the local reference system of link l to the local reference system of link $l-1$,

$\mathbf{T}^{(c,l)}$ – homogeneous transformation matrix from the local coordinate system of link l to reference system $\{0\}$,

$\mathbf{H}^{(c,l)}$ – pseudo-inertia matrix of link (c,l),

$\mathbf{r}_C^{(c,l)}$ – vector of position of the mass center of link l in chain c defined in its local reference system,

$\mathbf{J}$ – reducing matrix, $\mathbf{J} = \begin{bmatrix} \mathbf{j}_1 \\ \mathbf{j}_2 \\ \mathbf{j}_3 \end{bmatrix} = \begin{bmatrix} 1 & 0 & 0 & 0 \\ 0 & 1 & 0 & 0 \\ 0 & 0 & 1 & 0 \end{bmatrix}$,

$\mathbf{S}^{(c,l,s)}, \mathbf{D}^{(c,l,s)}$ – stiffness and damping matrices of $\mathrm{sde}(c,l,s)$, respectively,

$\mathbf{M}^{(c)}$ – mass matrix of the chain c,

$\mathbf{f}^{(c)}$ – vector of external, Coriolis, centrifugal and deformation forces acting in the chain c,

$\mathbf{e}^{(c)}$ – vector of dynamic forces,

$\mathbf{f}_l$ – vector of deformation forces of the flexible links,

$\mathbf{s}_c$ – vector of forces resulting from impacts in clearance joints,

$r^{(j)}, r^{(b)}$ – radius of the journal and bearing, respectively,

1 Introduction

Increased computational capabilities of modern computers allow us to simulate the dynamics of spatial linkages, taking into account the complex phenomena associated with their movement such as flexibility of links, friction and clearance in joints. There are many papers which deal with the issue of modelling dynamics of linkages or in general multibody systems [1-4]. The clearance in joints are especially dangerous. It can lead to abnormal loading of the linkage and as result to damage to the system. Among the other effects caused by the clearance in joints can be additional vibrations, noise and faster wear of parts. Simulations of dynamics of linkages with clearance in joints can be applied to the predict and assess the magnitude of the loads acting on the system.

In the literature it can be found many papers which deal with models of clearance of revolute joints [5-12], cylindrical joints [13], translational joints [14] or spherical joints [15-16]. A survey of analytical, numerical, and experimental approaches for the kinematics and dynamics analyses of multibody mechanical systems with clearance joints is presented in [5]. This work focuses on the modelling of linkages with clearance in revolute joints therefore, in the further part of the review, papers related only to revolute joints clearance model will be analyzed. Comparative study of clearance effects on dynamic behavior of planar linkages with clearance in revolute joints is shown in [6]. Proposed there the numerical model is validated by comparison with results obtained from experiment. The planar model of linkages with multiple revolute clearance joints is formulated in [7], whereas the planar model of revolute joints based on a geometric description of contact conditions and on a continuous contact force model is shown in [8]. In [9] is developed the spatial model of the revolute joint in which only radial clearance is taken into account. The cartesian coordinates are used in description of colliding bodies and the dynamics of the joint is controlled by contact–impact forces. Marques et al. in their works [10,11] extend model provided by Flores et al. [8, 9] by introducing axial clearance. In the paper [10] the Dahl and LuGre dynamics friction models are applied to model friction phenomenon. Akhadkary et al [12] analyse the influence of the joint clearance in a circuit breaker, which is a forty-two degrees of freedom linkage, on dynamic response of the system. In this paper, the spatial model of revolute joint with both radial and axial clearance taking into account contact with flanges is proposed. This model has been successfully validated by comparison with experimental data.

The aim of the paper is to develop automatic method generation of dynamics equations of motion of linkages whose links can be flexible and clearance together with friction in joint are taken into account. In the paper, it is assumed that the kinematics of linkage is described by means of the joint coordinates and homogeneous transformation matrices. Due to the adopted type of coordinates, in further consideration, it is assumed that the clearance can occur only in joints in which closed-loop kinematic chains are cut. The models of clearance presented in the paper are based on models presented in [8-9]. Friction in joint is modeled in the sense of the LuGre model [17-18]. The flexibility of links is modelled by means of the Rigid Finite Element Method (RFEM) [4]. The main advantage of the RFEM is the ability of application of the rigid-body formalism to model dynamics of the multibody systems with flexible links. This method has been successfully used to investigate dynamics of spatial linkages, manipulators, cranes, satellites [19-21].

The paper is organized as follows. In section 2 general introduction to linkages' topologies is presented. In the next section dynamics equations of motion of the RSUP linkage are derived. In the model presented there, it is assumed that all joints are ideal. Section 3 develops two models of the clearance, planar and spatial, which are formulated for the cut-joint of the RSUP linkage. In section 4 simulation results obtained for the linkage with rigid/flexible coupler and clearance in joint are presented. Results calculated for the linkage with ideal joint are also shown. The paper ends with conclusions and a list of references.

2 Topologies of linkage

In the general case kinematic structure the linkage can be open- or closed-loop (Fig. 1). Open-loop systems can form serial (Fig. 1a) or tree structure (Fig. 1c). When closed-loop kinematic chains are analysed, it is necessary to convert such a system into an equivalent system with an open-loop kinematic structure. In the paper the cut-joint technique is used in order to make such conversion. As a result, the spanning tree thus obtained can also have a serial (Fig. 1b) or tree structure (Fig. 1d). In the joint coordinates the dynamics equations of motion, depending on the kinematic structure of the linkage, can take one of the following forms:

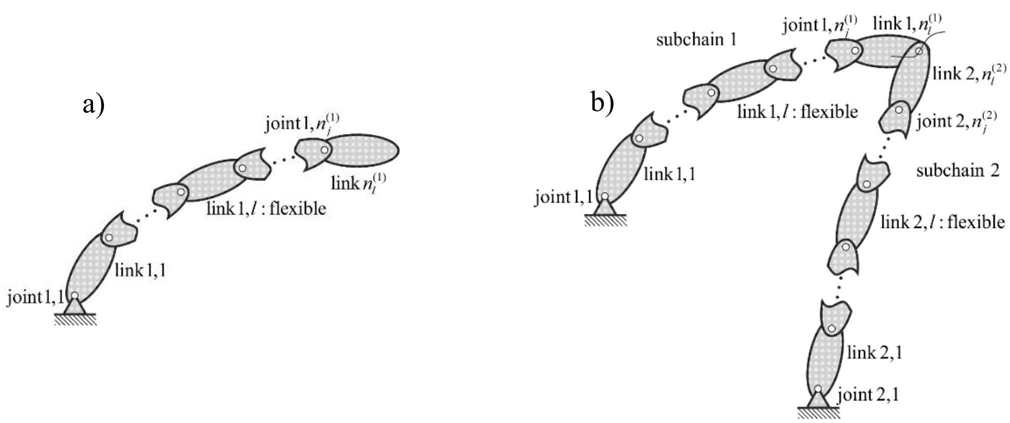

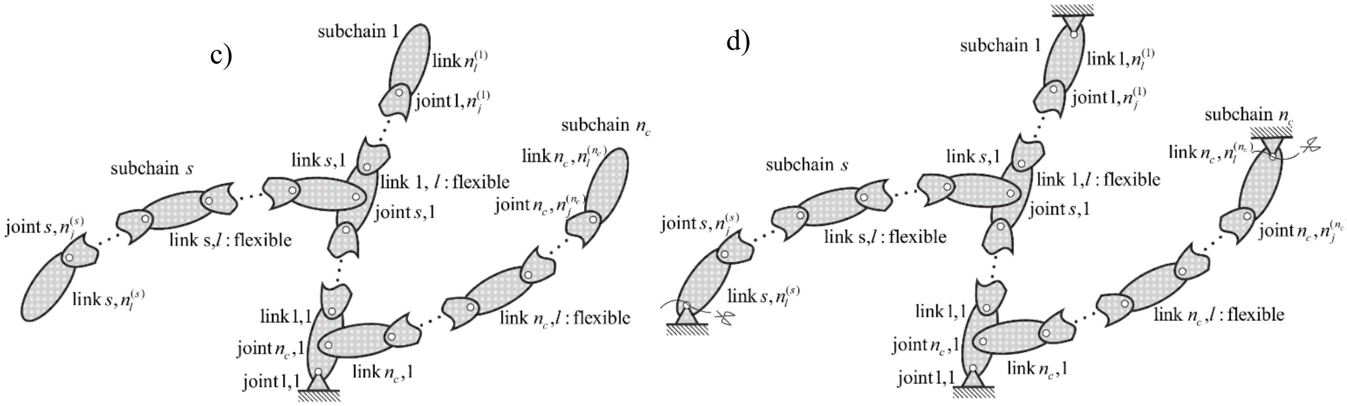

Fig. 1: Possible topologies of linkages

- the open-loop serial structure:

$$\mathbf{M}^{(1)}\ddot{\mathbf{q}} = \mathbf{f}^{(1)} \tag{1}$$

- the closed-loop serial structure:

$$\begin{bmatrix} \mathbf{M}^{(1)} + \mathbf{M}^{(2)} & -\boldsymbol{\Phi}_{\mathbf{q}}^T \\ \boldsymbol{\Phi}_{\mathbf{q}} & \mathbf{0} \end{bmatrix} \begin{bmatrix} \ddot{\mathbf{q}} \\ \boldsymbol{\lambda} \end{bmatrix} = \begin{bmatrix} \mathbf{f}^{(1)} + \mathbf{f}^{(2)} \\ \mathbf{c} \end{bmatrix} \tag{2}$$

- the open-loop tree structure:

$$\left(\mathbf{M}^{(1)} + \ldots + \mathbf{M}^{(s)} + \ldots + \mathbf{M}^{(n_c)}\right)\ddot{\mathbf{q}} = \left(\mathbf{f}^{(1)} + \ldots + \mathbf{f}^{(s)} + \ldots + \mathbf{f}^{(n_c)}\right) \tag{3}$$

- the closed-loop tree structure:

$$\begin{bmatrix} \mathbf{M}^{(1)} + \ldots + \mathbf{M}^{(s)} + \ldots + \mathbf{M}^{(n_c)} & -\boldsymbol{\Phi}_{\mathbf{q}}^T \\ \boldsymbol{\Phi}_{\mathbf{q}} & \mathbf{0} \end{bmatrix} \begin{bmatrix} \ddot{\mathbf{q}} \\ \boldsymbol{\lambda} \end{bmatrix} = \begin{bmatrix} \mathbf{f}^{(1)} + \ldots + \mathbf{f}^{(s)} + \ldots + \mathbf{f}^{(n_c)} \\ \mathbf{c} \end{bmatrix} \tag{4}$$

where: $\mathbf{M}^{(1)} = \begin{bmatrix} \mathbf{M}_{1,1}^{(1)} & \ldots & \mathbf{0} & \ldots & \mathbf{0} \\ \vdots & \ddots & & & \\ \mathbf{0} & \ldots & \mathbf{0} & \ldots & \mathbf{0} \\ \vdots & & & \ddots & \\ \mathbf{0} & \ldots & \mathbf{0} & \ldots & \mathbf{0} \end{bmatrix}, \mathbf{M}^{(s)} = \begin{bmatrix} \mathbf{M}_{1,1}^{(s)} & \ldots & \mathbf{M}_{1,s}^{(s)} & \ldots & \mathbf{0} \\ \vdots & \ddots & & & \\ \mathbf{M}_{1,s}^{(s)} & \ldots & \mathbf{M}_{s,s}^{(s)} & \ldots & \mathbf{0} \\ \vdots & & & \ddots & \\ \mathbf{0} & \ldots & \mathbf{0} & \ldots & \mathbf{0} \end{bmatrix}, \mathbf{M}^{(n_c)} = \begin{bmatrix} \mathbf{M}_{1,1}^{(n_c)} & \ldots & \mathbf{0} & \ldots & \mathbf{M}_{1,n_c}^{(n_c)} \\ \vdots & \ddots & & & \\ \mathbf{0} & \ldots & \mathbf{0} & \ldots & \mathbf{0} \\ \vdots & & & \ddots & \\ \mathbf{M}_{1,n_c}^{(n_c)} & \ldots & \mathbf{0} & \ldots & \mathbf{M}_{n_c,n_c}^{(n_c)} \end{bmatrix},$

$\mathbf{f}^{(1)} = \begin{bmatrix} \mathbf{f}_1^{(1)^T} & \ldots & \mathbf{0} & \ldots & \mathbf{0} \end{bmatrix}^T, \quad \mathbf{f}^{(s)} = \begin{bmatrix} \mathbf{f}_1^{(s)^T} & \ldots & \mathbf{f}_s^{(s)^T} & \ldots & \mathbf{0} \end{bmatrix}^T, \quad \mathbf{f}^{(n_c)} = \begin{bmatrix} \mathbf{f}_1^{(n_c)^T} & \ldots & \mathbf{0} & \ldots & \mathbf{f}_{n_c}^{(n_c)^T} \end{bmatrix}^T,$

$\mathbf{q} = \begin{bmatrix} \mathbf{q}^{(1)^T} & \ldots & \mathbf{q}^{(s)^T} & \ldots & \mathbf{q}^{(n_c)^T} \end{bmatrix}^T.$

Summarizing when the joint coordinates are applied and a linkage has open-loop kinematic structure the motion of the system is described by minimal set of coordinates. In the case of closed-loop systems closing constraint equations have to be formulated for each cut-joint.

3 Mathematical model of the RSUP linkage with ideal joints

A spatial one-dof RSUP linkage [22] consisting of four links is shown in Fig.1. It is assumed that the driving link is loaded by driving ($\mathbf{t}_{dr}^{(1,1)}$) and resistance ($\mathbf{t}_{res}^{(1,1)}$) torques, respectively. It is assumed that link $(2,2)$ (coupler) can be flexible and other links are rigid. The linkage is divided in the place of cut-joint R (revolute joint), and it leads to two open-loop kinematic chains: 1 – formed by links $(1,1)$, $(1,2)$ and 2 – formed by links $(2,1)$, $(2,2)$ (Fig.2). It is assumed that the clearance and friction occur only in cut-joint R.

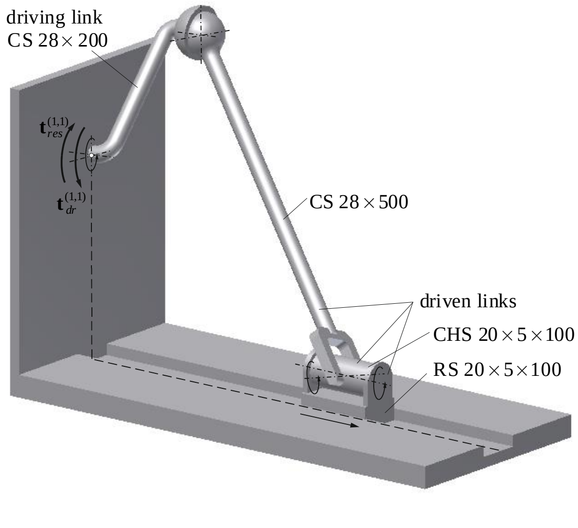

Fig. 2: RUSP linkage

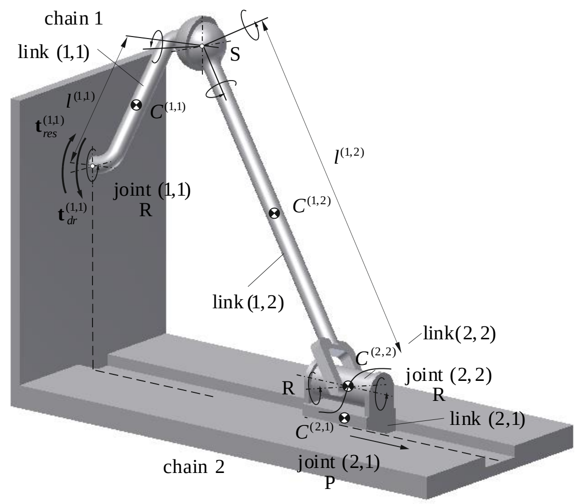

Fig. 3: Cut-joint technique

The Denavit-Hartenberg notation is used to define the motion of the linkage [23]. The RFEM is applied to model the flexibility of the coupler (Fig. 3). As a result the flexible link is replaced by the system of rigid elements (rfe) interconnected by means of spring-damping elements (sde) [4,20-21].

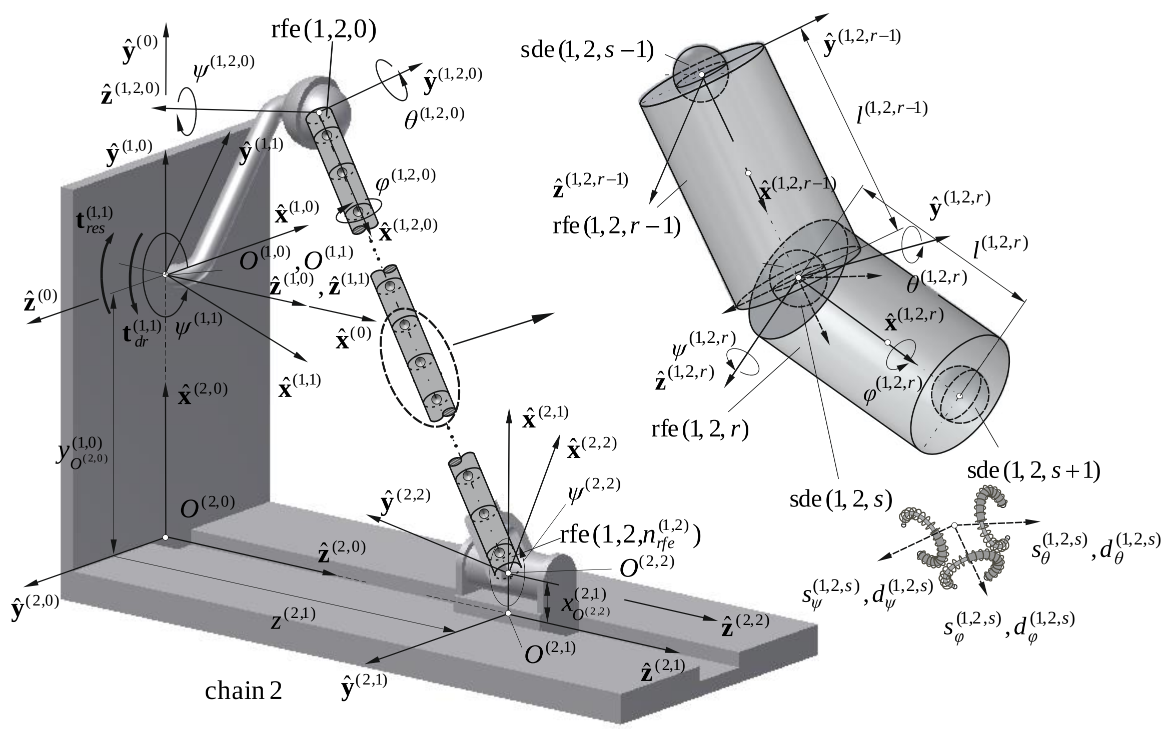

Fig. 4: The kinematics of the RSUP linkage

The motion of chains are defined by the vectors of generalized coordinates (joint coordinates) in the following form:

$$\mathbf{q}^{(c)}\Big|_{c=1,2} = \left(q_i^{(c)}\right)_{i=1,\dots,n_{dof}^{(c)}}, \tag{5}$$

where:

1) for chain 1: $\mathbf{q}^{(1)} = \left[\tilde{\mathbf{q}}^{(1,1)^T} \quad \tilde{\mathbf{q}}^{(1,2)^T}\right]^T$,

$$\tilde{\mathbf{q}}^{(1,1)} = \left[\psi^{(1,1)}\right],\quad \tilde{\mathbf{q}}^{(1,2)} = \begin{cases} \tilde{\mathbf{q}}^{(1,2,0)^T} & \text{if} \quad n_{rfe}^{(1,2)} = 1 \\ \left[\tilde{\mathbf{q}}^{(1,2,1)^T} \quad \cdots \quad \tilde{\mathbf{q}}^{(1,2,r)^T} \quad \cdots \quad \tilde{\mathbf{q}}^{(1,2,n_{rfe}^{(1,2)})^T}\right]^T & \text{if} \quad n_{rfe}^{(1,2)} > 1 \end{cases},$$

$$\tilde{\mathbf{q}}^{(1,2,r)}\Big|_{r=0,\dots,n_{rfe}^{(1,2)}} = \left[\psi^{(1,2,r)} \quad \theta^{(1,2,r)} \quad \varphi^{(1,2,r)}\right]^T,$$

2) for chain 2: $\mathbf{q}^{(2)} = \left[\tilde{\mathbf{q}}^{(2,1)^T} \quad \tilde{\mathbf{q}}^{(2,2)^T}\right]^T$,

$\tilde{\mathbf{q}}^{(2,1)} = \left[z^{(2,1)}\right]$, $\tilde{\mathbf{q}}^{(2,2)} = \left[\psi^{(2,2)}\right]$.

The homogeneous transformation matrices from the local reference frame attached to body l in kinematic chain c to the global reference frame $\{0\}$ are determined as follows:

$$\mathbf{T}^{(c,l)}\Big|_{\substack{c=1,2 \\ l=1,\dots,n_l^{(c)}}} = \mathbf{T}^{(c,l-1)}\tilde{\mathbf{T}}^{(c,l)}, \tag{6}$$

where:

1) for chain 1:

$$\tilde{\mathbf{T}}^{(1,0)} = \begin{bmatrix} 0 & 0 & 1 & 0 \\ 0 & 1 & 0 & 0 \\ -1 & 0 & 0 & 0 \\ 0 & 0 & 0 & 1 \end{bmatrix},\quad \tilde{\mathbf{T}}^{(1,1)} = \begin{bmatrix} \mathrm{c}\psi^{(1,1)} & -\mathrm{s}\psi^{(1,1)} & 0 & 0 \\ \mathrm{s}\psi^{(1,1)} & \mathrm{c}\psi^{(1,1)} & 0 & 0 \\ 0 & 0 & 1 & 0 \\ 0 & 0 & 0 & 1 \end{bmatrix},$$

$$\tilde{\mathbf{T}}^{(1,2)} = \begin{bmatrix} \mathrm{c}\psi^{(1,2)}\mathrm{c}\theta^{(1,2)} & \mathrm{c}\psi^{(1,2)}\mathrm{s}\theta^{(1,2)}\mathrm{s}\varphi^{(1,2)} - \mathrm{s}\psi^{(1,2)}\mathrm{c}\varphi^{(1,2)} & \mathrm{c}\psi^{(1,2)}\mathrm{s}\theta^{(1,2)}\mathrm{c}\varphi^{(1,2)} + \mathrm{s}\psi^{(1,2)}\mathrm{s}\varphi^{(1,2)} & 0 \\ \mathrm{s}\psi^{(1,2)}\mathrm{c}\theta^{(1,2)} & \mathrm{s}\psi^{(1,2)}\mathrm{s}\theta^{(1,2)}\mathrm{s}\varphi^{(1,2)} + \mathrm{c}\psi^{(1,2)}\mathrm{c}\varphi^{(1,2)} & \mathrm{s}\psi^{(1,2)}\mathrm{s}\theta^{(1,2)}\mathrm{c}\varphi^{(1,2)} - \mathrm{c}\psi^{(1,2)}\mathrm{s}\varphi^{(1,2)} & l^{(1,1)} \\ -\mathrm{s}\psi^{(1,2)} & \mathrm{c}\theta^{(1,2)}\mathrm{s}\varphi^{(1,2)} & \mathrm{c}\theta^{(1,2)}\mathrm{c}\varphi^{(1,2)} & 0 \\ 0 & 0 & 0 & 1 \end{bmatrix},$$

2) for chain 2:

$$\tilde{\mathbf{T}}^{(2,0)} = \begin{bmatrix} 0 & 0 & 1 & 0 \\ 1 & 0 & 0 & -y_{O^{(2,0)}}^{(1,0)} \\ 0 & 1 & 0 & 0 \\ 0 & 0 & 0 & 1 \end{bmatrix}, \tilde{\mathbf{T}}^{(2,1)} = \begin{bmatrix} 1 & 0 & 0 & 0 \\ 0 & 1 & 0 & 0 \\ 0 & 0 & 1 & z^{(2,1)} \\ 0 & 0 & 0 & 1 \end{bmatrix},\ \tilde{\mathbf{T}}^{(2,2)} = \begin{bmatrix} \mathrm{c}\psi^{(2,2)} & -\mathrm{s}\psi^{(2,2)} & 0 & x_{O^{(2,2)}}^{(2,1)} \\ \mathrm{s}\psi^{(2,2)} & \mathrm{c}\psi^{(2,2)} & 0 & 0 \\ 0 & 0 & 1 & 0 \\ 0 & 0 & 0 & 1 \end{bmatrix},$$

$\mathrm{s}\alpha^{(\beta,\gamma)} = \sin\alpha^{(\beta,\gamma)}$, $\mathrm{c}\alpha^{(\beta,\gamma)} = \cos\alpha^{(\beta,\gamma)}$.

The dynamics equations of motion for each kinematic chain of the unconstrained linkage are formulated using the Lagrange equations of the second kind [24]:

$$\frac{\mathrm{d}}{\mathrm{d}t}\frac{\partial E_k^{(c)}}{\partial \dot{\mathbf{q}}^{(c)}} - \frac{\partial E_k^{(c)}}{\partial \mathbf{q}^{(c)}} + \frac{\partial E_p^{(c)}}{\partial \mathbf{q}^{(c)}} = \mathbf{Q}^{(c)}, \tag{7}$$

where $E_k^{(c)} = \sum_{l=1}^{n_l^{(c)}} E_k^{(c,l)}$, $E_p^{(c)} = E_{p,g}^{(c)} + E_{p,f}^{(c)} = \sum_{l=1}^{n_l^{(c)}} E_{p,g}^{(c,l)} + \sum_{l=1}^{n_f^{(c)}} E_{p,f}^{(c,l)}$.

Components of the Lagrange equations are obtained using the computational approach presented in [4]. These equations are supplemented by the Lagrange multipliers and constraint equations formulated for joint in which closed-loop kinematic chain is divided. Finally the dynamics equations of motion of the RSUP linkage with ideal joints take a form:

$$\begin{bmatrix} \mathbf{M} & -\mathbf{\Phi}_{\mathbf{q}}^T \\ \mathbf{\Phi}_{\mathbf{q}} & \mathbf{0} \end{bmatrix} \begin{bmatrix} \ddot{\mathbf{q}} \\ \boldsymbol{\lambda} \end{bmatrix} = \begin{bmatrix} \mathbf{Q} - \mathbf{e} - \mathbf{f}_l \\ \boldsymbol{\gamma} \end{bmatrix}, \tag{8}$$

where:

$$\mathbf{M} = \begin{bmatrix} \mathbf{M}^{(1)} & \mathbf{0} \\ \mathbf{0} & \mathbf{M}^{(2)} \end{bmatrix},\ \ddot{\mathbf{q}} = \begin{bmatrix} \ddot{\mathbf{q}}^{(1)} \\ \ddot{\mathbf{q}}^{(2)} \end{bmatrix},\ \mathbf{e} = \begin{bmatrix} \mathbf{e}^{(1)} \\ \mathbf{e}^{(2)} \end{bmatrix},$$

$$\mathbf{M}^{(c)} = \begin{bmatrix} \mathbf{M}_{1,1}^{(c)} & \cdots & \mathbf{M}_{1,j}^{(c)} & \cdots & \mathbf{M}_{1,n_l^{(c)}}^{(c)} \\ \vdots & \ddots & \vdots & \iddots & \vdots \\ \mathbf{M}_{i,1}^{(c)} & \cdots & \mathbf{M}_{i,j}^{(c)} & \cdots & \mathbf{M}_{i,n_l^{(c)}}^{(c)} \\ \vdots & \iddots & \vdots & \ddots & \vdots \\ \mathbf{M}_{n_l^{(c)},1}^{(c)} & \cdots & \mathbf{M}_{n_l^{(c)},j}^{(c)} & \cdots & \mathbf{M}_{n_l^{(c)},n_l^{(c)}}^{(c)} \end{bmatrix},\ \mathbf{M}_{i,j}^{(c)} = \sum_{l=\max\{i,j\}}^{n_l^{(c)}} \tilde{\mathbf{M}}_{i,j}^{(c,l)},$$

$$\tilde{\mathbf{M}}_{i,j}^{(c,l)}\Big|_{i,j=1,\dots,l} = \left(\tilde{m}^{(c,l)}_{n_{dof}^{(c,i-1)}+v,\,n_{dof}^{(c,j-1)}+w}\right)_{\substack{v=1,\dots,\tilde{n}_{dof}^{(c,i)} \\ w=1,\dots,\tilde{n}_{dof}^{(c,j)}}},\ \tilde{m}_{i,j}^{(c,l)} = \mathrm{tr}\left\{\mathbf{T}_i^{(c,l)}\mathbf{H}^{(c,l)}\mathbf{T}_j^{(c,l)^T}\right\},\ \mathbf{T}_i^{(c,l)} = \frac{\partial \mathbf{T}^{(c,l)}}{\partial q_i^{(c,l)}},$$

$$\mathbf{e}^{(c)} = \begin{bmatrix} \mathbf{e}_1^{(c)} \\ \vdots \\ \mathbf{e}_i^{(c)} \\ \vdots \\ \mathbf{e}_{n_l^{(c)}}^{(c)} \end{bmatrix},\ \mathbf{e}_i^{(c)} = -\sum_{l=i}^{n_l^{(c)}} \left(\tilde{\mathbf{h}}_i^{(c,l)} + \tilde{\mathbf{g}}_i^{(c,l)}\right),$$

$$\tilde{\mathbf{h}}_i^{(c,l)}\Big|_{i=1,\dots,l} = \left(\tilde{h}^{(c,l)}_{n_{dof}^{(c,i-1)}+v}\right)_{v=1,\dots,\tilde{n}_{dof}^{(c,l)}},\ \tilde{h}_i^{(c,l)} = \sum_{m=1}^{n_{dof}^{(c,l)}} \sum_{n=m}^{n_{dof}^{(c,l)}} \mathrm{tr}\left\{\mathbf{T}_i^{(c,l)}\mathbf{H}^{(c,l)}\mathbf{T}_{m,n}^{(c,l)^T}\right\}\dot{q}_m^{(c,l)}\dot{q}_n^{(c,l)},\ \mathbf{T}_{m,n}^{(c,l)} = \frac{\partial^2 \mathbf{T}^{(c,l)}}{\partial q_m^{(c,l)}\partial q_n^{(c,l)}},$$

$$\tilde{\mathbf{g}}_i^{(c,l)}\Big|_{i=1,\dots,l} = \left(\tilde{g}^{(c,l)}_{n_{dof}^{(c,i-1)}+v}\right)_{v=1,\dots,\tilde{n}_{dof}^{(c,i)}},\ \tilde{g}_i^{(p)} = m^{(c,l)} g\ \mathbf{j}_2 \mathbf{T}_i^{(c,l)} \mathbf{r}_C^{(c,l)},$$

$$\mathbf{Q} = \begin{bmatrix} \mathbf{Q}^{(1)} \\ \mathbf{Q}^{(2)} \end{bmatrix} = \begin{bmatrix} \mathbf{t}_{dr}^{(1)} - \mathbf{t}_{res}^{(1)} \\ \mathbf{0} \end{bmatrix},\ \mathbf{t}_{dr}^{(1)} = \begin{bmatrix} t_{dr}^{(1,1)} \\ \mathbf{0} \end{bmatrix},\ \mathbf{t}_{res}^{(1)} = \begin{bmatrix} t_{res}^{(1,1)} \\ \mathbf{0} \end{bmatrix},$$

$$\mathbf{f}_l = \begin{bmatrix} \mathbf{f}_l^{(1)} \\ \mathbf{0} \end{bmatrix},\ \mathbf{f}_l^{(1)} = \begin{bmatrix} \mathbf{0} & \mathbf{S}^{(1,2)}\tilde{\mathbf{q}}^{(1,2)} \end{bmatrix},\ \mathbf{S}^{(1,2)} = \begin{bmatrix} \mathbf{S}^{(1,2,1)} & \mathbf{0} & \mathbf{0} \\ \mathbf{0} & \ddots & \mathbf{0} \\ \mathbf{0} & \mathbf{0} & \mathbf{S}^{(1,2,n_{sde}^{(1,2)})} \end{bmatrix},$$

$$\mathbf{\Phi}_{\mathbf{q}} = \frac{\partial \mathbf{\Phi}}{\partial \mathbf{q}},\ \boldsymbol{\gamma} = -\dot{\mathbf{\Phi}}_{\mathbf{q}}\dot{\mathbf{q}},\ \boldsymbol{\lambda} = \begin{bmatrix} f_{R,x} & f_{R,y} & f_{R,z} & n_{R,x} & n_{R,y} \end{bmatrix}^T,$$

$\mathbf{\Phi}(\mathbf{q}) = \mathbf{0}$ -holonomic constraint equations.

In simulations the Baumgarte stabilization method [25] is applied to eliminate constraint violations at the position and velocity level. Therefore, the right sides of the constraint equations have to be written in stabilized form as follows:

$$\boldsymbol{\gamma} = -\dot{\mathbf{\Phi}}_{\mathbf{q}}\dot{\mathbf{q}} - 2\alpha\dot{\mathbf{\Phi}} - \beta^2\mathbf{\Phi}, \tag{9}$$

where α and β are the stablization coefficients.

4 Dynamics of the RSUP linkage with clearance in joints

Due to the fact that the motion of the RSUP linkage's links is described in the joint coordinates the clearance is considered only in the cut-joint. It is assumed that the clearance exists only in rotational joints, and two models of the clearance, planar and spatial, are proposed. In both models only a radial clearance is taken into account and the influence of the axial clearance is neglected.

In the case of the planar model, it is assumed that the axes of the connected links are parallel, and the contact forces acting between the contacting surfaces are the same along the connection axis. Let us consider two bodies bearing b and journal j which represent two joined links (Fig. 4).

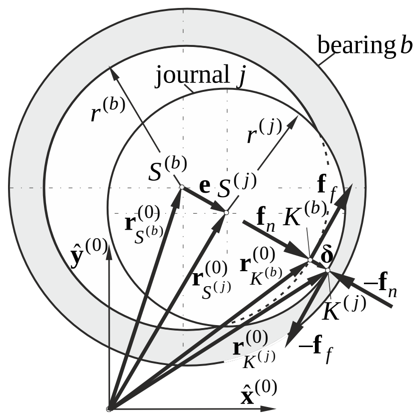

Fig. 5: The planar model of the clearance

The radial clearance between joints can be calculated as:

$$c_r = r^{(b)} - r^{(j)} \tag{10}$$

The eccentricity vector $\mathbf{e}$ which describes relative position between the journal and the bearing center can be given by:

$$\mathbf{e} = \mathbf{r}^{(0)}_{S^{(b)}} - \mathbf{r}^{(0)}_{S^{(j)}}. \tag{11}$$

Depending on the magnitude of the eccentricity vector, two phases of motion can be considered:

$\|\mathbf{e}\| < c_r$ - no contact exists between the journal and bearing and no forces are introduced into dynamics equations of motion,

$\|\mathbf{e}\| \geq c_r$ - contact exists and two forces are introduced into system: normal contact force, determined from an impact force law, and friction forces calculated using bristles' friction models.

The penetration depth causes by the impact of the connected links can be calculated as:

$$\delta = \|\mathbf{e}\| - c_r. \tag{12}$$

The impact force $\mathbf{f}_n$ acting between the journal and bearing is evaluated using the model proposed by Lankarani and Nikravesh [26] and it is given by:

$$\|\mathbf{f}_n\| = K\delta^n \left(1 + \frac{3\left(1-k_e^{\,2}\right)}{4}\frac{\dot{\delta}}{\dot{\delta}^{(-)}}\right), \tag{13}$$

where K is the generalized stiffness, n is the exponent equals to 1.5 for metal surfaces, k_e is the restitution coefficient and $\dot{\delta}^{(-)}$ is the velocity in the initial impact phase. The contact model (13) is extension of the classical Hertz contact law and it allows us to take into account energy dissipation introduced by a damping hysteretic factor.

The tangent force $\mathbf{f}_f$ corresponds to the friction force which is modelled by means of the LuGre bristles' friction model [17,18]. Therefore, the friction coefficient can be expressed as follows:

$$\mu = \sigma_0 z + \sigma_1 \dot{z} + \sigma_2 v_t , \tag{14}$$

where v_t is the tangent velocity, σ_0, σ_1, σ_2 are stiffness, damping and viscous damping coefficients which describe the contact of the bristle, respectively.

Deflection of the bristle z can be calculated from the additional state equation which can be written in the following form:

$$\dot{z} = v_t \left(1 - \frac{\sigma_0 z \operatorname{sgn}(v_t)}{\mu_k + (\mu_s - \mu_k) \exp\left(-\left(\frac{v_t}{v_s} \right)^2 \right)} \right), \tag{15}$$

where μ_s, μ_k are static and kinetic friction coefficients, respectively.

Total force acting in the contact point can be expressed as the sum of the normal and tangent forces:

$$\mathbf{f}_c = \mathbf{f}_f + \mathbf{f}_n . \tag{16}$$

The generalized forces associated with contact force $\mathbf{f}_c$ are given by:

$$\mathbf{s}_c = \mathbf{f}_c^{\,T} \frac{\partial \mathbf{r}^{(0)}_{K^{(b)}}}{\partial \mathbf{q}} - \mathbf{f}_c^{\,T} \frac{\partial \mathbf{r}^{(0)}_{K^{(j)}}}{\partial \mathbf{q}} . \tag{17}$$

The dynamics equations of motion of the RSUP linkage with the planar model of clearance in the cut-joint can be rewritten in the following form:

$$\begin{bmatrix} \mathbf{M} & -\mathbf{\Phi}^T_{\mathbf{q},p} \\ \mathbf{\Phi}_{\mathbf{q},p} & \mathbf{0} \end{bmatrix} \begin{bmatrix} \ddot{\mathbf{q}} \\ \boldsymbol{\lambda}_p \end{bmatrix} = \begin{bmatrix} \mathbf{Q} - \mathbf{e} - \mathbf{f}_l + \mathbf{s}_c \\ \boldsymbol{\gamma}_p \end{bmatrix} , \tag{18}$$

where $\boldsymbol{\lambda}_p = \begin{bmatrix} f_{R,z} & n_{R,x} & n_{R,y} \end{bmatrix}^T$ are the Lagrange multipliers. The constraint equations $\mathbf{\Phi}_p(\mathbf{q}) = \mathbf{0}$ describes that the axis of rotation of the bearing and journal should be parallel and connected bodies can't move along this axis.

In the case of a spatial model, skewing of the axis additionally is taken into account. The influence of the axial clearance is neglected.

In the paper following scenarios of the contact are considered:

- no contact exists between connected links,
- the bearing and journal are in contact along the line,
- the journal contacts with bearing at a point
- both links are in contact in two points (Fig.6).

Applying reasoning similar to that presented for the planar model, dependencies for forces acting at the contact points can be derived. Thus, the generalized forces vector can be expressed as:

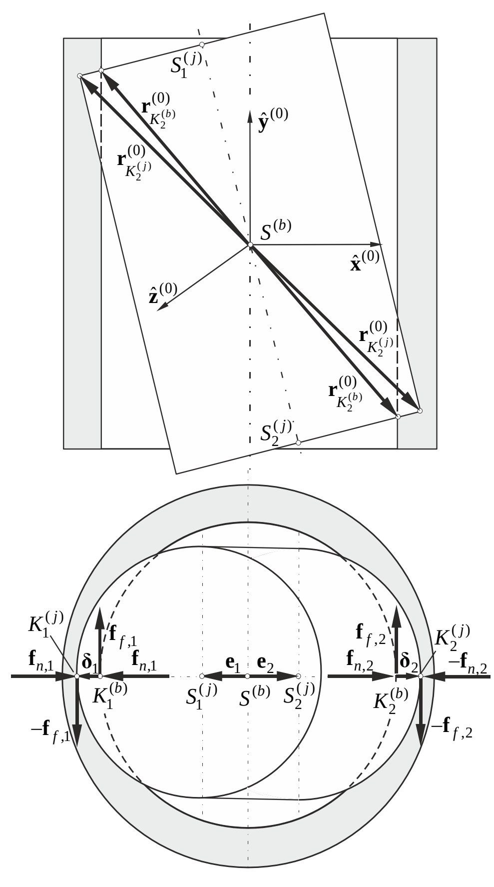

Fig. 6: The spatial model of the clearance

$$\mathbf{s}_c = \mathbf{f}_{c,1}{}^T \frac{\partial \mathbf{r}^{(0)}_{K_1^{(b)}}}{\partial \mathbf{q}} + \mathbf{f}_{c,2}{}^T \frac{\partial \mathbf{r}^{(0)}_{K_2^{(b)}}}{\partial \mathbf{q}} - \mathbf{f}_{c,1}{}^T \frac{\partial \mathbf{r}^{(0)}_{K_1^{(j)}}}{\partial \mathbf{q}} - \mathbf{f}_{c,2}{}^T \frac{\partial \mathbf{r}^{(0)}_{K_2^{(j)}}}{\partial \mathbf{q}} . \tag{19}$$

Finally introducing of the spatial model of clearance into the mathematical model of the RSUP linkage lead to the following equations of motion:

$$\begin{bmatrix} \mathbf{M} & -\mathbf{\Phi}^T_{\mathbf{q},s} \\ \mathbf{\Phi}_{\mathbf{q},s} & \mathbf{0} \end{bmatrix} \begin{bmatrix} \ddot{\mathbf{q}} \\ \boldsymbol{\lambda}_s \end{bmatrix} = \begin{bmatrix} \mathbf{Q} - \mathbf{e} - \mathbf{f}_l + \mathbf{s}_c \\ \boldsymbol{\gamma}_s \end{bmatrix} , \tag{20}$$

where $\boldsymbol{\lambda}_s = \left[f_{R,z} \right]^T$ is the reaction force acting along the joint axis which results from the constraint equation $\mathbf{\Phi}_s(\mathbf{q}) = \mathbf{0}$ according to which the joined links can't move along this axis.

5 Numerical simulations

In simulations, it is assumed that stable value of the driving torque is $t^{(1,1)}_{dr,0} = 10\,\text{Nm}$ and this value is reached in time $t_s = 2\,\text{s}$. The angular velocity of the crank corresponding to the resistance torque $t^{(1,1)}_{res,0} = t^{(1,1)}_{dr,0}$ is $\dot{\psi}^{(1,1)}_0 = 9$ rad s^{-1} (Fig. 7).

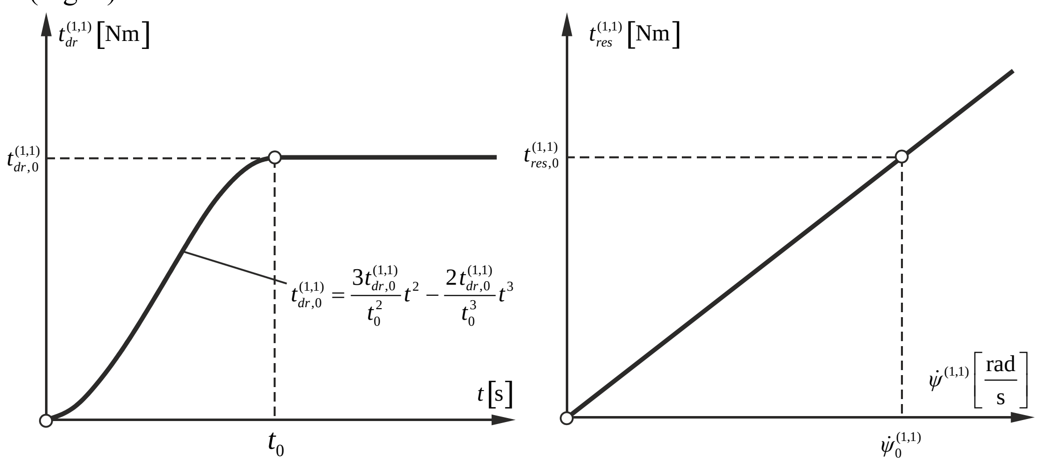

Fig. 7: Assumed courses of driving and resistance torques

The initial configuration of the linkage is described by the following vector:

$$\mathbf{q} = \Bigg[\underbrace{\frac{\pi}{2}}_{\tilde{\mathbf{q}}^{(1,1)}} \quad \underbrace{0 \quad 0 \quad -\frac{\pi}{3}}_{\tilde{\mathbf{q}}^{(1,2,0)}} \quad \underbrace{\mathbf{0}}_{\tilde{\mathbf{q}}^{(1,2,1)}} \quad \ldots \quad \underbrace{\mathbf{0}}_{\tilde{\mathbf{q}}^{(1,2,n^{(1,2)}_{rfe})}} \quad \underbrace{0.25}_{\tilde{\mathbf{q}}^{(2,1)}} \quad \underbrace{0}_{\tilde{\mathbf{q}}^{(2,2)}} \Bigg]^T . \tag{18}$$

The flexible coupler was discretized into 5 rfes. The parameters applied in simulation are summarized in Tab. 1. The dynamics equations were integrated using the Runge-Kutta method of fourth order with constant step size equals to $h = 5 \cdot 10^{-6}\,\text{s}$. The Baumgarte stabilization coefficients applied in simulation were $\alpha = 100$, $\beta = 50$.

Table 1: Parameters applied in simulations

Parameter	Symbol	Value
Static coefficient of the friction	μ_s	0.2

Kinetic coefficient of friction	μ_k	0.1
Stribeck velocity, $\mathrm{m\,s^{-1}}$	v_s	0.0175
Stiffness coefficient, $\mathrm{m^{-1}}$	σ_0	600
Damping coefficient, $\mathrm{s\,m^{-1}}$	σ_1	$\sqrt{600}$
Coefficient of viscosity, $\mathrm{s\,m^{-1}}$	σ_2	0
Radius of the bearing, m	$r^{(b)}$	0.005
Radius of the journal, m	$r^{(j)}$	0.004
Coefficient of restitution	k_e	0.9

The influence of the clearance on the motion of the linkage can be observed through the time courses of the slider displacement, velocity and acceleration (Fig. 8). In the time courses of the slider velocity, it can be observed slight peaks caused by the influence of the impulse forces. It can be seen, that the clearance significantly affects on acceleration courses. Magnitude of the acceleration is significantly larger than the one obtained for the ideal joint. Fig. 9 shows time courses of the contact force acting in the clearance joint obtained for model with rigid and flexible coupler. It can be noted, that the number of peaks caused by the impact force is also larger when the coupler is flexible (Fig. 8). Similar conclusion can be formulated for the time courses of the acceleration.

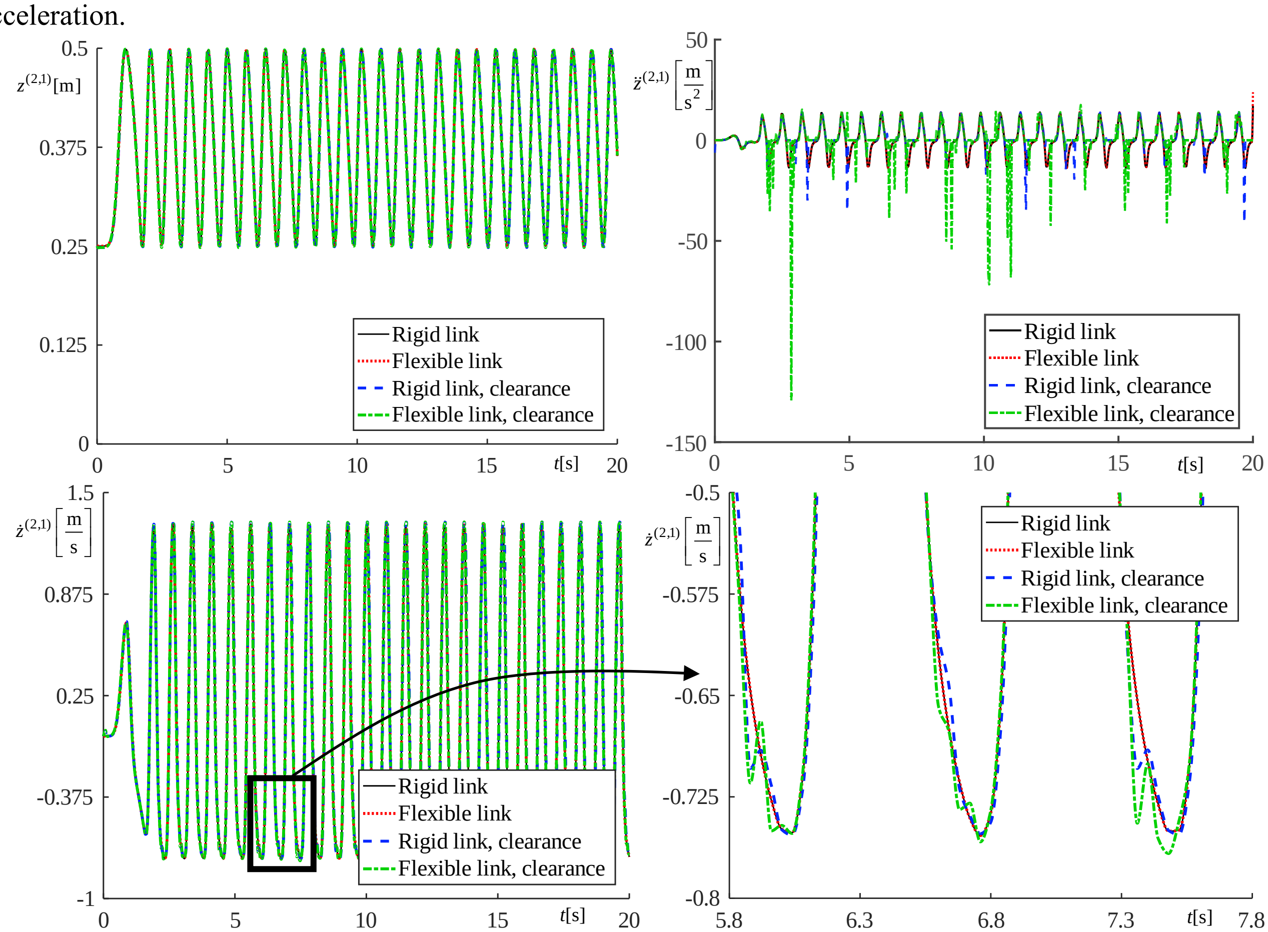

Fig. 8: Time courses of values of displacement, velocity and acceleration of the slider

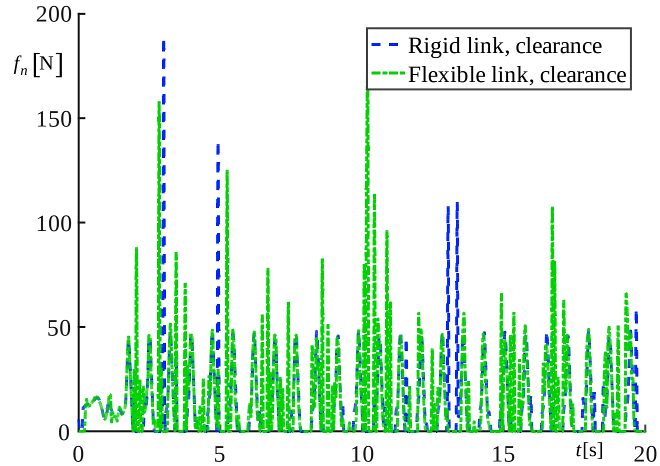

Fig. 9: Time courses of values of the normal contact force

Trajectory of the journal inside the bearing is presented in Fig. 10. Black dotted line represents the reference circle whose radius equals to the assumed clearance in joint (1mm). Each crossing of this reference line means that the journal and bearing are in contact.

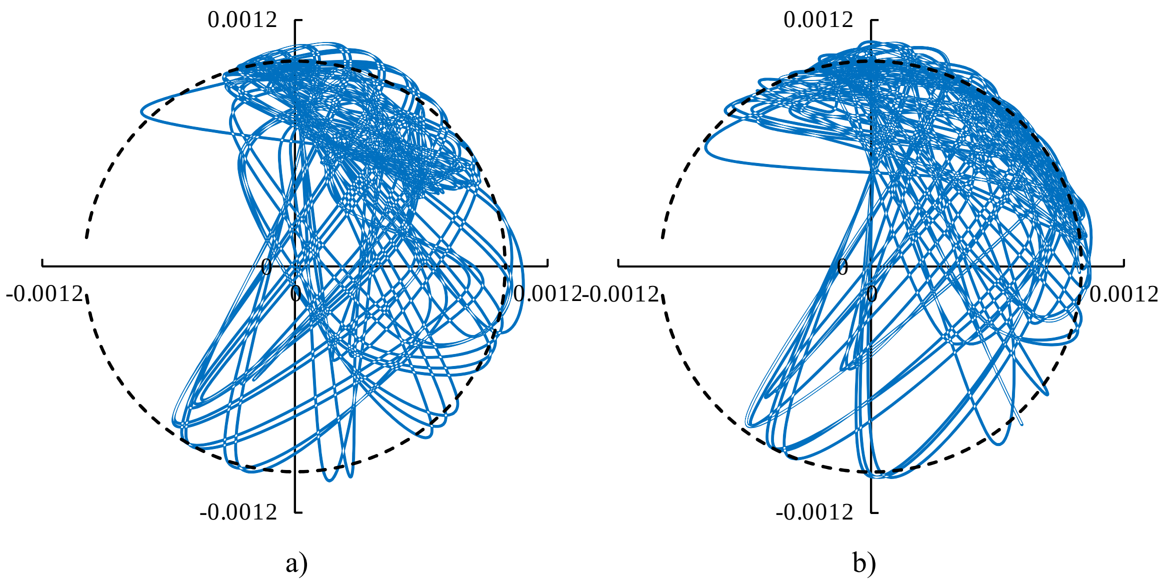

Fig. 10: Journal trajectory obtained for linkage with rigid (a) and flexible (b) coupler

6 Conclusions

Dynamics model of the spatial linkage with flexible links and clearance in revolute joints was presented. The joint coordinates and homogeneous transformation matrices were applied in description of motion of the links. Due to this fact the clearance effect was analyzed only in joints in which closed-loop chain was divided into open-loop kinematic chains. The planar and spatial models of clearance were proposed. Both models use the normal contact force model based on the Lankarani–Nikravesh contact force model and friction phenomenon is modeled by means of the LuGre friction model. Flexible links were discretized by means of the RFEM. As a special case of the spatial linkage, dynamics of the RSUP linkage was analyzed. In numerical simulations, dynamic response of the system with/without clearance and with/without flexible links were analyzed. Only results obtained for planar model of the clearance were presented. Simulations show that the clearance has the significant influence on motion of the linkage and force acting in joints. For the assumed geometric dimensions of the linkage, the link flexibility have no a great influence on the system dynamic response. The flexibility affects the number of impulses caused by the contact of the journal and bearing. In the extended version of this work will be presented the detailed formulas leading to the determination of the contact forces. Results obtained for the spatial model will be also shown.

Acknowledgements

This paper is realized within the research project number 2017/01/X/ST8/01978 funded by the Polish National Science Centre.

References

[1] A. A. Shabana, *Dynamics of Multibody Systems*, Wiley, New York, 1989.

[2] P.E. Nikravesh, *Computer-Aided Analysis of Mechanical Systems*, Prentice Hall, 1988.

[3] J.G. de Jalón, E. Bayo, *Kinematic and Dynamic Simulation of Multibody Systems*, The Real-Time Challenge, Springer-Verlag, New-York, 1994.

[4] E. Wittbrodt, M. Szczotka, A. Maczyński, S. Wojciech, Rigid *Finite Element Method in Analysis of Dynamics of Offshore Structures.* Ocean Engineering & Oceanography, Springer, Berlin-Heidelberg, 2013.

[5] Q. Tian, P. Flores, H.M. Lankarani, "A comprehensive survey of the analytical, numerical and experimental methodologies for dynamics of multibody mechanical systems with clearance or imperfect joints," *Mechanism and Machine Theory*, 122, pp. 1–57, 2018.

[6] Y. Chen, Y. Sun, B. Peng, C. Cao, "A comparative study of joint clearance effects on dynamic behavior of planar multibody mechanical systems," *Latin American Journal of Solids and Structures*, 13, pp. 2815-2833, 2016.

[7] J. Ma, L. Qian, "Modelling and simulation of planar multibody systems considering multiple revolute clearance joints," *Nonlinear Dyn*, 90, pp. 1907–1940, 2017.

[8] P. Flores, J. Ambrósio, "Revolute joints with clearance in multibody systems," *Computers & Structures*, 82, pp.1359-1369, 2004.

[9] P. Flores, J. Ambrósio, J.C. Pimenta Claro, H.M. Lankarani, "Spatial revolute joints with clearance for dynamic analysis of multibody systems," in *Proceedings of the Institution of Mechanical Engineers, Part K: Journal of Multi-body Dynamics*, Vol. 220, Issue 4, pp. 257–271, 2006.

[10] F. Marques, D. Rychecký, F. Isaac, M. Hajžman, P. Polach, P. Flores, "Spatial Revolute Joints with Clearance and Friction for Dynamic Analysis of Multibody Mechanical Systems," in *Proceedings of the 4th Joint International Conference on Multibody System Dynamics*, Montréal, Canada, May 29 – June 2, 2016.

[11] F. Marques, F. Isaac, N. Dourado, P. Flores, "An enhanced formulation to model spatial revolute joints with radial and axial clearance," *Mechanism and Machine Theory*, 116, pp. 123-144, 2017.

[12] N. Akhadkar, V. Acary, B. Brogliato, "Multibody systems with 3D revolute joints with clearance: an industrial case study with an experimental validation," *Multibody System Dynamics*, 42, 3, pp. 249–282, 2018.

[13] C. Liu, Q. Tian, H. Hu, "Dynamics and control a spatial rigid-flexible multibody system with multiple cylindrical clearance joints," *Mechanism and Machine Theory*, 52, pp. 106-129, 2012.

[14] L. Wu, D.B. Marghitu, J. Zhao, "Nonlinear Dynamics Response of a Planar Mechanism with Two Driving Links and Prismatic Pair Clearance," Mathematical Problems in Engineering, 2017, https://doi.org/10.1155/2017/4295805.

[15] P. Flores, H.M. Lankarani, “Spatial rigid-multibody systems with lubricated spherical clearance joints: modelling and simulation,” *Nonlinear Dyn*, 60, pp. 99–114, 2010.

[16] F. Marques, F. Isaac, N. Dourado, A.P. Souto, “A study on the dynamics of spatial mechanisms with frictional spherical clearance joints,” in *Proceedings of the ASME 2016 International Design Engineering Technical Conferences & Computers and Information in Engineering Conference IDETC/CIE 2016*, Charlotte, North Carolina, USA , August 21-24, 2016.

[17] C. Canudas de Wit, H. Ollson, K.J. Åström, P. Lischinsky, “A new model for control of systems with friction,” *IEEE Trans. Autom. Control*, 40, 3, pp. 419–425, 1995.

[18] K. Augustynek, A. Urbaś, “Comparison of bristles' friction models in dynamics analysis of spatial linkages,” *Mechanics Research Communications*, 2017, doi: 10.1016/j.mechrescom.2017.01.003.

[19] M. Szczotka, “A modification of the rigid finite element method and its application to the J-lay problem,” *Acta Mechanica*, vol. 220, no. 1, pp. 183-198, 2011.

[20] A. Urbaś, “Computational implementation of the rigid finite element method in the statics and dynamics analysis of forest cranes,” *Applied Mathematical Modelling*, 2016, http://dx.doi.org/10.1016/j.apm.2016.08.006.

[21] K. Augustynek, A. Urbaś, “Two approaches of the rigid finite element method to modelling the flexibility of spatial linkage links,” in *Proceedings of the 8th ECCOMAS Thematic Conference on Multibody Dynamics 2017*, June 19-22, Prague, 2017.

[22] O.A. Bauchau, J. Changkuan, “Modelling friction phenomena in flexible multibody dynamics,” *Comput. Methods Appl. Mech. Eng*., 195, pp. 6909–6924, 2006.

[23] J.J. Craig, *Introduction to Robotics Mechanics and Control*, Addison-Wesley Publishing Company, Inc., 1989.

[24] E.I. Jurevič, *Dynamics of Robot Control*. Nauka In:, 1984; Moscow. (in Russian)

[25] J.W. Baumgarte, “Stabilization of constraints and integrals of motion in dynamical systems,” *Computer Methods in Applied Mechanics and Engineering*, 1, 1, pp. 1–16, 1972.

[26] H.M. Lankarani, P.E. Nikravesh, “A contact force model with hysteresis damping for impact analysis of multibody systems,” *J. Mech. Des.* 112, 3, pp. 369–376, 1990.